JACS
JOURNAL OF THE AMERICAN CHEMICAL SOCIETY

ARTICLE

pubs.acs.org/JACS

Oxidative Nucleophilic Substitution of Hydrogen in the Sapphyrin Dioxouranium(VI) Complex: A Relativistic DFT Study

Grigory A. Shamov*

Department of Chemistry, University of Manitoba, Winnipeg, Manitoba, Canada, R3T 2N2

Kazan State Technology University, Centre for New Information Technologies, K.Marks str. 68, Kazan 420015, Russian Federation

Supporting Information

ABSTRACT: A potentially trianionic expanded porphyrin ligand, sapphyrin does not form a 1:1 complex with the uranyl cation. However, in the presence of methanol, a complex of uranyl and meso-methoxy-substituted iso-sapphyrin is formed [Burrel et al. J. Chem. Soc., Chem. Commun. 1991, 24, 1710]. Here we performed a relativistic DFT study on the thermodynamics and the possible mechanism of the reaction. Our results have shown that (1) the reason for the failure of sapphyrin to stabilize its 1:1 uranyl complex is the highly basic character of the trianionic form of ligand that is hard to achieve in solution, (2) a driving force for the reaction lies in the better affinity of the methanol-substituted (and isomerized) ligand dianion to the uranyl cation, compared with the unsubstituted sapphyrin dianion, and (3) for the single-stage synchronous methanol addition pathways explored in this work, there is a path corresponding to noninnocent uranium behavior, via a neutral, triplet U(IV) intermediate complex. However, if the solvation effects were taken into account, this pathway would be unfavorable compared with singlet U(VI) pathways involving anionic intermediate complexes. The later pathway can be described as classical oxidative nucleophilic substitution of hydrogen in an aromatic system.

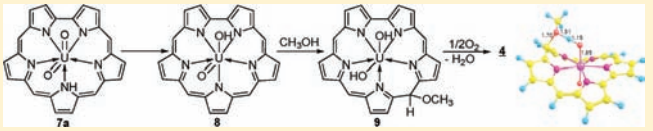

INTRODUCTION

Recently, expanded porphyrins (porphyrin-like macrocycles containing more than four pyrrole moieties)[1] have been considered as prospective agents for the complexation of actinide cations, notably actinyls, with important potential applications in nuclear waste remediation. Several systems capable of coordinating actinyls effectively were described. The progress in this field has been reviewed.[2,3]

22-Pentaphyrin[1,1,1,1,0][4] or sapphyrin, **1** (Chart 1), was the very first macrocycle within the expanded porphyrin family, first described in the 1960s by Woodward.[5] Its 22-electron conjugated π-system allows consideration of the sapphyrin as an aromatic compound. The inner cavity size and shape of sapphyrin should be very similar to those of 22-pentaphyrin[1,1,1,1,1], which is known to form stable uranyl complexes.[6] Moreover, a recent experimental study shows that oxasapphyrin forms a uranyl complex **3** readily.[7] At the same time, sapphyrin, being a potentially trianionic ligand, does not form the 1:1 uranyl complex **2**; the ligand either returns unchanged or decomposes. However, in the presence of methanol and air, a uranyl complex **4** yields rapidly.[6] The compound **4** is a complex of the dianionic ligand **5**, which can be considered as a product of substitution of one of the meso-hydrogens of iso-sapphyrin **6** by a methoxy group.

In the original experimental work,[6] heating a mixture of free sapphyrin **1** and methanol in pyridine/triethylamine solution for 72 h does not lead to substitution. However, after the addition of a uranyl salt, the reaction completes in 2 h giving the complex **4**. One can guess that a uranyl−sapphyrin complex forms and then reacts with methanol. Therefore, this reaction is a rare and interesting example of the introduction of a nucleophilic substituent into the meso-bridge of an aromatic expanded porphyrin complex. In the absence of oxygen, the reaction leads to a different uranium complex, which can be separated from the reaction mixture. Being exposed to oxygen, it gives the same product **4**. This fact was interpreted[6] as proof that this intermediate contains the methoxy moiety already. Based on these findings, the following reaction mechanism was proposed that includes formation of auranium(IV) complex **9**, as shown in eq 1.

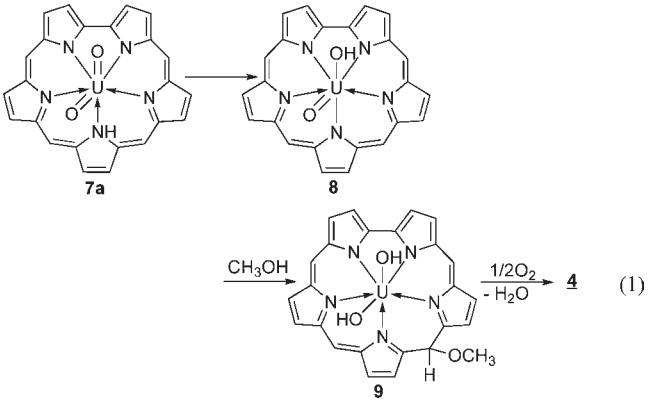

(1)

In the following years, there has been considerable progress in the understanding of the nucleophilic substitution of hydrogen in

Received: July 23, 2010
Published: March 07, 2011

Chart 1. Sapphyrin and Its Derivatives and Complexes Considered in This Paper

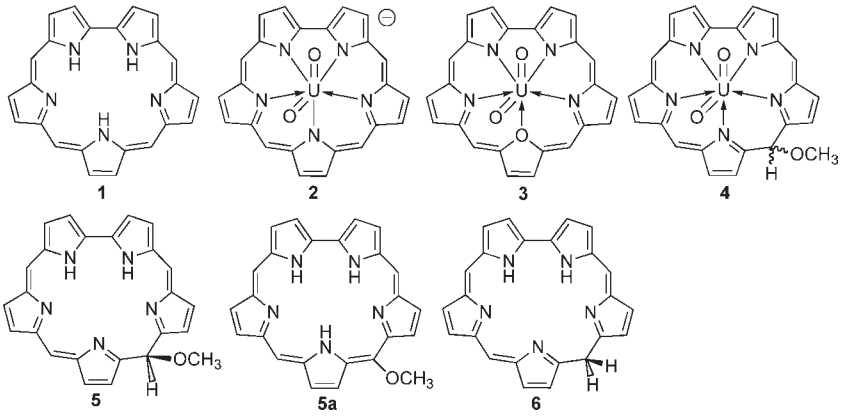

classical aromatic compounds (cf. the review by Makosza[8]). It is well-known that aromatic nucleophilic substitution reactions go through a "σ-complex" intermediate. In the case of hydrogen substitution, the formation of the corresponding σ^H complex is a fast process, but because the hydride ion is a bad leaving group, the substitution reaction can only take place if this hydrogen is removed from the σ^H complex with the help of an additional reagent (eq 2). One of the most typical cases of hydrogen removal is oxidation by another reagent. This process is described by the authors of ref 8 as "oxidative nucleophilic substitution of hydrogen" (ONSH).

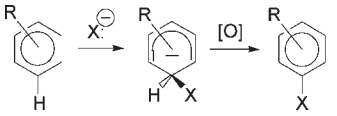

(2)

The introduction of the methoxy group to the sapphyrin ligand can be described as ONSH in the meso-bridge of the aromatic expanded porphyrin system with uranium(VI) as the oxidizing agent. In uranyl chemistry, this would be usually considered atypical, but recent experimental, as well as theoretical, studies have shown that some participation of uranyl in reactions, as well as functionalization of the uranyl oxo-ligands, can happen;[9−11] see also refs 12−16,17. However, by analogy with the usual organic aromatic compounds, one can guess another possibility, that the uranyl dication within the ligand, acting as a strong electron-withdrawing group, would stabilize the σ^H-complex of the aromatic expanded porphyrin ligand without changes in the oxidation state of the uranium atom, and the ligand then gets oxidized by the oxygen.

Quantum-chemical studies of this reaction could help in understanding the role played by the actinide cation in its mediation. In the present work, we will employ relativistic density functional theory (DFT) calculations to answer the following questions: (1) Why does sapphyrin fail to form a 1:1 uranyl complex, while oxasapphyrin does form it? (2) What is the driving force of the methoxylation process, which includes the break of aromaticity of the sapphyrin ring, and why does the last stage, that is, the oxidation by oxygen, not restore the aromaticity of sapphyrin? (3) What is the role of uranium in this nucleophilic substitution? Is it just a strong electron-withdrawing group allowing nucleophilic attack onto the sapphyrin ring or a non-innocent metal changing its oxidation state during the process?

The structure of the present paper will be as follows. First, reagents, the uranyl oxasapphyrin complex **3** and the final reaction product **4**, will be considered. These complexes were characterized by IR and X-ray spectroscopy in the original work,[6] and therefore, can be used for testing the adequacy of our computational method. Next, we will discuss the thermodynamics of the substitution process. Then, possible isomers of complexes of dianionic sapphyrin with dioxouranium(VI) will be discussed, along with the corresponding methanol adducts like compound **9** and its isomers. Finally, possible reaction pathways of the methanol addition will be examined.

COMPUTATIONAL DETAILS

Modeling actinide complexes of expanded porphyrins is a difficult task because of the importance of both correlation and relativistic effects for these systems.[18,19] Moreover, the size of plausible model systems all but prohibits the use of wave function-based correlation methods. Therefore, the only practical method of treatment for these systems is density functional theory (DFT).[20] DFT is a single-determinant method and, as such, might have problems with the treatment of nondynamic correlation and spin−orbit effects. The latter effects are indeed important in systems containing f-electrons like complexes of uranium(IV). However, previous experience[21−25] shows that it is possible to get their reaction energies, geometries of complexes, and vibrational spectra right, with acceptable accuracy, using scalar-relativistic methods and DFT, provided that the relativistic method is reasonably good.

In this work, the geometries of reagents, products, and transition states were fully optimized with the DFT program Priroda[26,27] version 3, using a scalar four-component relativistic method[28] employing the spin−orbit separation scheme by Dyall.[29] The finite nucleus model was used in these relativistic calculations. Unless otherwise noted, the PBE[30] density functional was used with all-electron Gaussian basis sets of triple-ζ polarized quality, labeled R3Z, as supplied with the Priroda code version 3. The large-component basis sets were accompanied by small-component basis sets obtained via the kinetic balance scheme.[28] Resolution of identity technique[31,32] was used throughout for both Coulomb and exchange integrals, using corresponding optimized fitting basis sets as supplied with the Priroda version 3. All stationary points were first located at the PBE/R3Z level. Unless otherwise noted, the energies in the text refer to PBE/R3Z results. For all the PBE/R3Z optimized structures, analytical second derivatives were calculated with the Priroda code; all minima had zero and all transition states had one negative Hessian eigenvalue. In most of the cases, intrinsic reaction coordinate calculations were performed to assert which reagents and products belong to a given transition state.

Recently, there were significant developments in understanding the accuracy and applicability of the DFT methods in general and, in particular, for the chemistry of porphyrin transition metal complexes. For the latter, significant evidence exists that for the accurate description of spin states of the porphyrin and corrole complexes, care should be

dx.doi.org/10.1021/ja106566g | J. Am. Chem. Soc. 2011, 133, 4316–4329

taken in the choice of the basis set and density functional. It was shown that ECP methods with sparsely contracted basis GTO-type sets often used in DFT might lead to significant inaccuracies,[33−35] and all-electron, smooth, correlation-consisted Gaussian basis sets with a large number of primitives are a necessity. For the spin splitting in transition metal complexes, particularly porphyrins and corroles, it was reported that density functionals based on the OPTX exchange[36] such as OLYP and OPBE can be significantly more accurate than other GGA and hybrids.[37−39] The OLYP functional has also been shown to often produce more accurate activation barriers compared with other pure GGA DFs.[40]

Thus for studying the role of density functionals in the description of the spin states of the complexes, we have reoptimized them with OLYP, as well as PBE, functionals using the large optimized correlation consistent cc-pVTZ-quality L2 relativistic basis set,[41] again with corresponding fitting and small-component basis sets using the Priroda code version 6. These data are labeled herein as OLYP/L2 and PBE/L2.

Earlier, we tested this code and relativistic method against thermodynamic and structural experimental data available for some small uranium fluorides, oxides,[23] and nitrates.[42] We also successfully employed it for calculations of hydration energies and redox potentials of actinyl ions,[43] modeling of oxygen exchange in uranyl under basic conditions,[44] and structures and bonding in expanded porphyrin actinyl complexes.[25,45−48] Other more recent studies comparing the Priroda results with other relativistic methods exist.[49]

Calculations of solvation effects and extended transition state (ETS) energy decomposition calculations[50−53] were performed with the ADF[54−57] program package as single-point calculations on geometries optimized within the Priroda code. Relativistic effects were taken into account using the ZORA[58−60] formalism. All ADF calculations were performed with the PBE density functional with all-electron ZORA-TZP Slater-type basis sets,[61] with frozen core approximation for the "small-core" orbitals. For the ETS computations, historically, ADF version 2004[62] has been used; solvation energy computations were done with the ADF 2010.[57] For a few selected cases, effects of the spin−orbit interactions on the energy differences were computed with the spin−orbit ZORA method in noncollinear open-shell approximation.[63−66]

To calculate solvation effects on reaction energies, the COSMO[67] continuum solvation model, as implemented[68] in ADF, was used for single-point calculations. Klamt[69] atomic radii for C, N, O, H, and Cl atoms were used; for the uranium atom, a radius of 1.70 Å was used. The particular choice of uranium radius is not really important because uranium does not contribute to the solvent-accessible surface. The pyridine solvent, as parametrized within the ADF 2010 code, was used throughout, in the self-consistent COSMO manner. In selected cases, in addition to the single-point ADF COSMO computations on the Priroda PBE/R3Z geometries, full geometry optimizations were performed. Effects on the geometries and energies were found to be small, so the reoptimization in solution has not been pursued further (see Supporting Information, Table S3).

All systems with unpaired electrons were treated using the unrestricted Kohn−Sham formalism.

Chart 2. Diastereomeric Forms of the Product 4

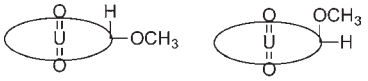

4a 4b

RESULTS AND DISCUSSION

1. Reagents and Final Products. Geometries of small molecules taking part in our reactions, namely, molecular oxygen, methanol, and water, are well-known. Various isomers of the free-base sapphyrin were calculated in the literature[70] with hybrid DFT methods. It was shown that the (normal) structure of the sapphyrin **1** is the most stable one, compared with the "inverted" isomers, as well as the isomers with different distribution of the NH hydrogens inside the macrocycle. Thus in this work, we considered only this isomer for sapphyrin **1**, as well as for the related oxasapphyrin **3**. We will always use unsubstituted ligands instead of the deca-alkyl-substituted ones studied experimentally. For the sake of simplicity, to calculate some of the reaction energies, we will use trimethylamine as the model base and *cis*-$(NMe_3)_2UO_2Cl_2$ complex as the reference uranyl source.

There are two possible diastereomeric forms of the addition product **4**. They differ by the orientation of the methoxy group with respect to the sapphyrin macrocycle, shown in Chart 2: one with an equatorial orientation (**4a**) and another with the axial orientation (**4b**).

These diastereomers can convert one into another by macrocyclic ring flipping. The process is reported to be slow at the NMR time scale. In the crystal lattice, these forms are present in a 70:30 ratio. In chloroform solution, they form an equimolar mixture of diastereomers.[6] These results are in agreement with the small energy difference given by our method; the Priroda PBE/R3Z calculations give **4a** as lying 3 kcal/mol below **4b**.

Calculated geometric parameters of **4a** and **4b** and the experimental ones of **4b** are shown in Table 1; the latter product is also shown on the Figure 2 below. The calculated and experimental geometries for the uranyl oxasapphyrin complex **3** are provided in the table as well. The PBE/R3Z geometries agree acceptably with the experiment, although the method systematically gives slightly longer uranyl bond lengths, as well as equatorial bond lengths, than the ones from the X-ray experiment. Asymmetric uranyl stretch frequencies of the complexes, given by our calculation, are in good agreement with the experimental values from IR spectra. We observed the same general type of agreement for the scalar

Table 1. Calculated and Experimental (Where Available) Bond Lengths, Å, and Uranyl Vibrational Frequencies, cm^{-1}, for DioxouVI) Complexes and Their Experimental Analogs[a]

complex	U=O	U−N1	U−N2	U−N3	U−N4	U−N5/O1	ν_{asym} (O=U=O)
2 calcd	1.804 (2.21)	2.562 (0.49)	2.650 (0.42)	2.570 (0.49)	2.650 (0.42)	2.562 (0.49)	922
3 calcd	1.795 (2.23)	2.485 (0.57)	2.610 (0.44)	2.641 (0.44)	2.485 (0.57)	2.830 (0.14)	942
3 expt[b]	1.768	2.449(3)	2.582(3)	2.587(3)	2.470(3)	2.791(3)	936
4a calcd	1.800 (2.18)	2.511 (0.50)	2.515 (0.50)	2.572 (0.44)	2.592 (0.42)	2.517 (0.47)	925
4b calcd	1.799; 1.796	2.528	2.525	2.594	2.539	2.604	937
4b expt[c]	1.727(10)	2.466(10)	2.492(10)	2.548(11)	2.515(12)	2.477(11)	919
7a calcd	1.796; 1.804 (2.21; 2.18)	2.484 (0.58)	2.484 (0.57)	2.681 (0.42)	2.824 (0.24)	2.680 (0.42)	927

[a] In parentheses are corresponding population bond orders. Numeration of atoms is in Scheme 1. [b] Reference 7. [c] Reference 6.

dx.doi.org/10.1021/ja106566g | J. Am. Chem. Soc. 2011, 133, 4316–4329

relativistic PBE calculations in our previous studies on the actinyl complexes of Schiff-base and expanded-porphyrin macrocyclic ligands.[45−47]

2. Uranyl Complexation Energies: ETS Analysis. In the original experimental paper,[6] the following explanation was put forward for the fact that sapphyrin fails to form a 1:1 in-cavity complex with uranyl: The ligand's inner cavity is not feasible for the coordination, or the higher charge of the trianionic form "might render it unsuitable for complexation." In our view, this statement deserves further scrutiny. In this section, we will analyze the stabilities of the following uranyl complexes: the anionic complex of the sapphyrin **2**, the neutral complex of the oxasapphyrin **3**, the neutral complex of one of the isomers of monoprotonated sapphyrin **7a**, and finally the complex **4**, product of the ONSH. Several ways of estimating the stability of a macrocyclic complex can be considered. One can determine the binding energy of the complex from the actinyl cation and ligand anion, as in eq 3:

$$UO_2^{2+} + L^{(n)-} \rightarrow UO_2L^{(2-n)-} \quad (3)$$

This approach has a potential disadvantage that comes from possible inaccuracies of treating the di- and trianions of the ligands with DFT methods, which methods are known to yield nonbound solutions for HOMO.[71,72] This could lead to an overestimation of the corresponding binding energies, and more so for the trianionic ligand than for the dianionic one. Therefore, a safer way to estimate the binding energies might be to avoid highly anionic species by using neutral uranium(IV) dioxide and ligand radicals (and anion radicals in the case of the complex **2**) as in eq 4:

$$UO_2^{(\bullet\bullet)} + L^{(\bullet\bullet)(2-n)-} \rightarrow UO_2L^{(2-n)-} \quad (4)$$

The complex binding energies by either eq 3 or 4, can be analyzed further using the methodology of the ETS decomposition scheme as follows.[50−53] First, the binding energy from the optimized cation and anion is broken down into the preparation energy, E_{prep}, which is the energy required to promote the cation and anion from their free state to the geometries (and electronic states, if needed) of the corresponding fragments in the complex, and the energy of interaction between the fragments, E_{int}. Then, the latter energy is partitioned down to the contributions of the Pauli repulsion (E_{Pauli}), electrostatic interactions (E_{Elstat}), and an "orbital interactions" term, E_{Orb}, which accounts for covalent and polarization energies between the fragments. The details and discussion of the ETS decomposition are provided in our previous work on the actinyl complexes of expanded porphyrins and Schiff-base macrocycles.[45,46] Here we follow the same methodology. For computational convenience, we chose the binding energy of the ionic fragments according to eq 3 for the ETS partition. The calculated energies and their components are provided in Table 2. We also include the radical energy by eq 4 in the table for comparison.

Scheme 1. Numeration of Atoms in Sapphyrin Ring Used Throughout the Paper

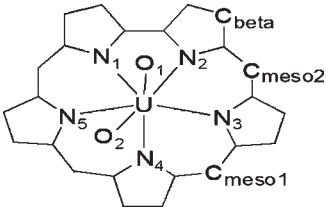

First, we note that the complex **2** of the sapphyrin trianion has a favorable binding energy with respect to both of the processes. For the eq 3, the binding energy obviously should be higher for any trianionic ligand than for the dianionic ones; however, even the radical process 4 for the trianionic sapphyrin is more exothermic than that for the oxasapphyrin **3**. The Pauli repulsion terms for the complexes **2** and **3** and the neutral monoprotonated sapphyrin **7a** are close to each other, which suggests that the steric requirements of the ligands' internal cores are quite similar.

Comparing two neutral complexes, the oxasapphyrin uranyl complex **3** with **7a**, we can see that the total energies of either process 3 or 4 are lower for the former one. The internal binding energies for these complexes are very similar. If we compare the bond orders for ligand donor atom to metal bonds (Table 1) for these complexes with the ones of **2**, we notice that for the furanic oxygen of the oxasapphyrin complex, as well as for the protonated pyrrolic nitrogen of the complex **7a**, distances to uranium are significantly longer and the bond orders are smaller than the corresponding ones in **2**. It shows that both protonation of the pyrrolic nitrogen and its substitution to oxygen have the same effect of breaking, or at least significantly weakening, the corresponding uranium−ligand bond. Analyzing the binding energy of the reaction components for reaction 3 provided in Table 2, one can see that the difference in the stabilities of complexes **3** and **7a** is due to significantly higher preparation energies for the latter, caused by unfavorable steric repulsion between the hydrogen on the pyrrolic nitrogen and the uranyl moiety within the ligand core (Figure 1).

On the basis of these gas-phase calculation results, we can conclude that there is nothing intrinsically "wrong" with the structure of the sapphyrin ligand itself; that is, there is nothing structurally that could possibly prevent it from forming a 1:1 complex with uranyl, at least if the ligand has all three NH-protons removed, as in the anionic complex **2**.

The substitution product **4** has more negative energies of both the "ionic" binding, eq 3, and the "radical" binding, eq 4, than the neutral complexes **3** and **7a**. (The radical reaction, eq 4, for **4** is even more exothermic than it is for the anionic complex **2**.) The main reason for this is a significantly more negative electrostatic energy for **4**, compared with both **3** and **7a**, with somewhat higher Pauli repulsion energies and lower E_{Orb} compensating

Table 2. Complex Binding Energies and Its ETS Decomposition[a]

complex UO_2L	radical binding energy [b], Priroda	ionic binding energy [c], Priroda	E_{prep} Priroda [d]	E_{Int} Priroda [d]	E_{Int} ADF [d]	E_{Pauli} [d]	E_{Elstat} [d]	E_{Orb} [d]
2	−213.7	−786.9	18.2	−805.0	−806.0	169.4	−708.3	−267.0
3	−197.3	−620.6	14.1	−634.8	−631.6	166.1	−542.1	−255.6
4a	−226.4	−634.1	19.3	−653.4	−653.0	201.9	−571.9	−283.1
7a	−175.3	−601.4	33.1	−634.5	−631.5	169.8	−537.9	−263.5

[a] All values in kcal/mol. [b] $UO_2^{(\bullet\bullet)} + L^{(2-n)(\bullet\bullet)} \rightarrow UO_2L^{(2-n)}$ [c] $UO_2^{2+} + L^{n-} \rightarrow UO_2L^{(2-n)}$ [d] $E(1) = E_{prep} + E_{Int}$; $E_{Int} = E_{Pauli} + E_{Elstat} + E_{Orb}$.

dx.doi.org/10.1021/ja106566g |J. Am. Chem. Soc. 2011, 133, 4316–4329

each other. These terms reflect the fact that the inner cavity of the substitution product is smaller than the ones of the original sapphyrins: the average U−N bond distances in complexes **4a**, **2**, and **7a** are 2.541, 2.599, and 2.631 Å, correspondingly. The finding is in line with our previous works on other uranyl complexes of expanded porphyrins,[45,46] where it was shown that the ligands' inner cavity is often too large and uranyl(VI) binding energy can be increased via contraction of the ligand by its "saddle"-like deformation.

Another possibility to assess the stability of a complex is to consider its formation reaction, in our case from the free-base ligand and a source uranyl complex. It is generally accepted that the process of formation of the porphyrin complexes does not include formation of highly charged species like the porphyrin dianion but goes via a series of equilibria involving partially protonated ligands and complexes.[73] Thus it is reasonable to assume, by analogy, that the formation of the uranyl−sapphyrin complex occurs via a series of similar equilibria as well, such as the one shown in eq 5.

$$[UO_2]^{2+} + LH_3 \rightarrow UO_2(LH_2)^+ \rightarrow UO_2LH \rightarrow UO_2L^- \quad (5)$$

Since we know that every protonation of nitrogen in the uranyl−sapphyrin complex significantly weakens the corresponding uranium to nitrogen bond and thus destabilizes the complex (see above), we will not consider the intermediate deprotonated cationic complex, $UO_2(LH_2)^+$, here. Starting from the uranyl dichloride complex with trimethylamine, a neutral complex can be obtained (again arbitrarily choosing isomer **7a** for the time being), as per eq 6.

$$UO_2Cl_2(NMe_3)_2 + \mathbf{1} \rightarrow \mathbf{7a} + 2Cl^- + NMe_3H^+ \quad (6)$$

Then the process of deprotonation of **7a** by an excess of trimethylamine has to be considered:

$$\mathbf{7a} + NMe_3 \rightarrow \mathbf{2} + NMe_3H^+ \quad (7)$$

In solution, the reaction 6 was found to be slightly endoergic (ΔG_{298} = +7 kcal/mol), while it was strongly endoergic in the gas phase (+239.7, correspondingly, due to high energy of the naked ions on the right-hand side of eq 6). The gas-phase and solution (pyridine) Gibbs free energies for reaction 7 are provided in Table 3. It is strongly endoergic in the gas phase due to the highly basic character of the trianionic sapphyrin and the obvious unfavorability of the charge separation in the gas phase. However, reaction 7 was found to be exoergic in solution, predicting the formation of a 1:1 anionic uranyl complex **2** as possible. This is contrary to the experimental observations that such a complex cannot be characterized. One possible explanation for the nonexistence of **2** is that the solid resulting from the combination of complex **2** and a counterion is likely to have a smaller dielectric constant than that of the pyridine solution. Thus it might not be enough to stabilize ionic pairs (charge

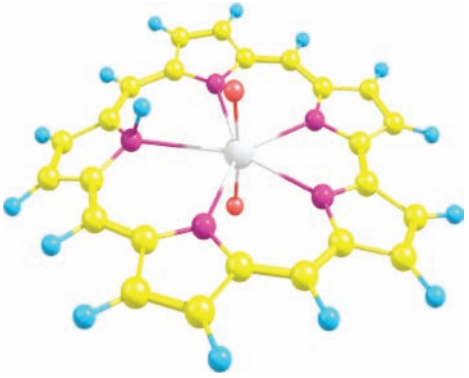

Figure 1. Complex **7a**, PBE/R3Z optimized geometry.

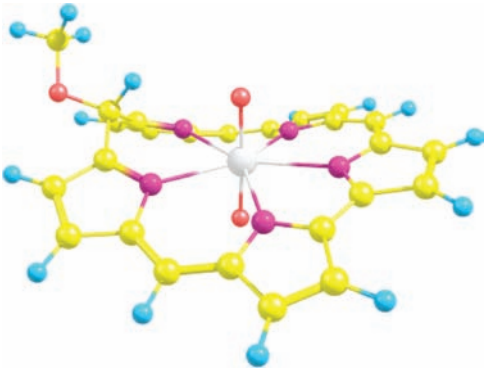

Figure 2. Complex **4**, PBE/R3Z optimized geometry.

Table 3. Thermodynamics of Reactions 7− Computed at PBE/R3Z Level for Gas-Phase and Pyridine Solution.[a]

eq	reaction	ΔE^{gas}	ΔG^{gas}_{298}	ΔG^{solv}_{298}
7	$\mathbf{7a} + NMe_3 \rightarrow \mathbf{2} + NMe_3H^+$	73.3 (73.9)	75.6	−12.7
8	$\mathbf{1} + CH_3OH + \frac{1}{2}O_2 \rightarrow \mathbf{5} + H_2O$	−9.0 (−10.1)	−3.4	−5.3
9	$\mathbf{7a} + CH_3OH + \frac{1}{2}O_2 \rightarrow \mathbf{4a} + H_2O$	−40.0 (−38.2)	−31.9	−35.6
10	$\mathbf{12a} + NMe_3 \rightarrow \mathbf{11b} + NMe_3H^+$	68.1 (66.9)	70.3	−18.8
11	$\mathbf{11b} + NMe_3 \rightarrow \mathbf{14} + NMe_3H^+$	146.4 (146.1)	146.7	0.4
12	$\mathbf{12a} + \frac{1}{2}O_2 \rightarrow \mathbf{4a} + H_2O$	−71.2 (−70.6)	−77.1	−85.7
13	$\mathbf{14} + 2NMe_3H^+ + \frac{1}{2}O_2 \rightarrow \mathbf{4a} + 2NMe_3 + H_2O$	−285.7 (−284.5)	−294.1	−67.3

[a] Solvation energies are taken from PBE/ZORA-TZP COSMO calculations. Gas-phase PBE/ZORA-TZP energy differences are in parentheses. All values are in kcal/mol.

dx.doi.org/10.1021/ja106566g | J. Am. Chem. Soc. 2011, 133, 4316–4329

separation) and prevent protonation of the ligand leading to a less stable complex of the **7a**-type. Thus there might be 1:1 in-cavity complexes of uranyl and the sapphyrin ligand in various degrees of protonation in polar solution but not in the less-polar solid state.

3. Reaction Thermodynamics, Driving Force of the Methoxylation Process. The energy required for the methoxylation reaction to break the aromaticity of the sapphyrin's cyclic conjugated π-system for the latter process can be roughly estimated as the energy of the isomerization of the sapphyrin **1** to a nonconjugated isomer, the iso-sapphyrin **6**. The isomerization was found to be a highly unfavorable process with gas-phase Gibbs free energy of +26.7 kcal/mol. Thus it is interesting to analyze what pays off the energy costs of the substitution reaction. To do that, we consider it for both free sapphyrin **1** and its neutral complex **7a** (eqs 8 and 9, correspondingly). Here we arbitrarily chose the neutral form **7a** as the source compound because the product **4a** on the right-hand side of eq 9 is also a neutral complex and thus no charge separation occurs during the process.

$$\mathbf{1} + CH_3OH + \frac{1}{2}O_2 \rightarrow \mathbf{5} + H_2O \qquad (8)$$

$$\mathbf{7a} + CH_3OH + \frac{1}{2}O_2 \rightarrow \mathbf{4a} + H_2O \qquad (9)$$

As one can see from the calculated gas-phase Gibbs free energies (Table 3), the oxidative substitution−isomerization reaction of the free sapphyrin **1** is mildly exothermic. Therefore, there is some driving force for this process in the formation of the very stable water molecule and a new C−O bond, which is enough to compensate the breaking of the aromaticity of the sapphyrin π-system. To estimate the cost of the breaking, we calculated the aromatic methoxy-substituted sapphyrin **5a** (shown on Chart 1); its free energy is 20.0 kcal/mol lower than the one of **5**.

For the uranyl complex **7a**, the reaction is much more exothermic than it is for the free ligand. The difference in these reaction energies (about 28 kcal/mol) is close to the differences between E_{Int} of the complexes **4** and **7a** (about 22 kcal/mol, see Table 2). Hence the higher stability of complex **4** is in large part due to the more favorable shape of the ligand's inner core, providing shorter uranium−nitrogen distances. Also, the hydrogen atom on a sapphyrin's meso-carbon does not have unfavorable steric interactions with the uranyl that the hydrogen sitting on N-donor atoms has.

4. Mechanism of the Reaction: Initial Uranyl Complexes. In this study, we took for granted that essential parts of the mechanism proposed in the original work of Sessler[6] are valid. That is, we assume that the reaction goes via some 1:1 sapphyrin complex with uranyl(VI) coordinated within the internal core of the ligand, with the subsequent addition of methanol to it. There is significant evidence that the mechanistic assumptions are valid. It can be justified by the available experimental data and partly by the results presented in the previous section. Considering first the experimental data, there is the evidence of the existence of an intermediate containing all three fragments, namely, methanol, sapphyrin, and uranium. Moreover, the available experimental data indicates the absence of any reaction if any one of these three components is missing. Regarding the results presented in the previous section, we have shown that the stability of complex **4** is the thermodynamic driving force of the process. Moreover, if the substitution could happen without formation of this complex, it would lead to a normal, nonisomerized meso-methoxy-sapphyrin **5a**, which is 20.0 kcal/mol more stable than compound **5**.

Chart 3. Isomeric Forms of the Neutral Uranyl−Sapphyrin Complex

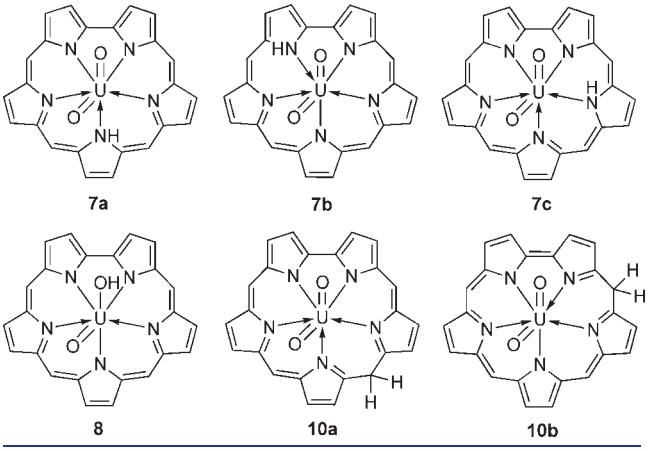

We also presume that the neutral form of methanol attacks this complex and the addition process proceeds in a synchronous way: while the oxygen of methanol connects to the meso-carbon of the sapphyrin ligand, the hydrogen from the methanol jumps to one of the neighboring donor atoms of the complex. Methanol dissociation under the experimental reaction conditions is unlikely (in water, pK_a of methanol is 16, while that of triethylamine is about 10.7; while this might change in the nonaqueous pyridine−methanol mixture, there still must be a strong preference to neutral methanol). It can be argued that since reaction 7 is highly endothermic in the gas phase, the methanol's proton would rather go somewhere on the ligand than to the solvent molecule or another trialkylamine. Perhaps a trimolecular mechanism involving more than one methanol molecule (or a combination of methanol and amine molecules) with a proton-shuttling type of mechanism cannot be completely excluded; but here we did not consider such cases.

There are several protonation sites possible for the neutral uranyl sapphyrin complex besides **7a**. Various nitrogen atoms (as in **7a**−**c**) and uranyl oxygen (as in **8**, which was considered in the original paper[6]) can be protonated (Chart 3). Moreover, it is known from the rich chemistry of the corrole,[74−76] which is the closest analog of sapphyrin among tetrapyrrolic porphyrins and can be considered the lower sapphyrin homologue, that the meso-carbon atoms can also be protonated (ref 1 and references therein), so it is necessary to consider structures **10a** and **10b** as well.

Indeed, Priroda PBE/R3Z calculations show that the most stable isomers are the meso-CH forms, especially **10a** (Table 4). Both NH forms, **7a** and **7b**, are of similar energy, while **7c** is slightly more stable than the two former ones. From Table 1, one can see that in all the sapphyrin and oxasapphyrin complexes, bonds between uranium and the nitrogens N3 and N5 are longer and of lower bond-order than the ones to N1, N2, and N4. Thus the protonation of the N3 and N5 nitrogens, which effectively breaks the bond to the uranium, destabilizes the complex to a slightly lesser degree. The OH form, **8**, is the least stable neutral uranyl sapphyrin isomer. The instability of **8** can be explained by a lower basicity of the uranyl oxygen compared with the equatorial nitrogens and by destabilization of the uranyl moiety

Table 4. Calculated Energies for Neutral Uranyl Sapphyrin Source Complexes and Their Interconversion Transition States, Relative to the Singlet Ground State of 7a[a]

structure/spin state	PBE/R3Z	PBE/L2	OLYP/L2	PBE/ZORA TZP, gas phase	PBE/ZORA TZP pyridine solution
7a/S	0.0	0.0	0.0	0.0	0.0
7a/T		25.5	23.6		
7b/S	0.3	0.1	1.0	0.4	0.3
7b/T		24.0	22.6	38.7	27.5
8/S	10.1	10.1	15.5	12.8	13.7
8/T		18.4	19.8		
10a/S	−7.1	−6.8	−5.8	−6.7	−7.4
10a/T	11.1	11.4	12.9	11.5	10.4
10b/S	−1.8	−1.5	−1.1		
10b/T		13.0	13.9		
TS **7a**−**8**/S	19.4	19.7	24.2	20.4	22.9
TS **7b**−**8**/S	18.0	17.9		19.8	21.3
TS **10a**−**8**/S	24.4	24.2	32.4	25.5	27.2
TS **10a**−**8**/T		46.8	53.1		
TS **7a**−**10a**/S	38.9	38.7	40.4	39.0	37.6
TS **7a**−**10a**/T		62.3	62.1		

[a] All values are in kcal/mol.

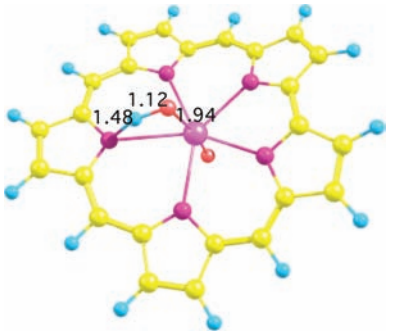

Figure 3. Transition state for **7a** to **8** isomerization, PBE/R3Z optimized geometry; selected bond lengths in Å.

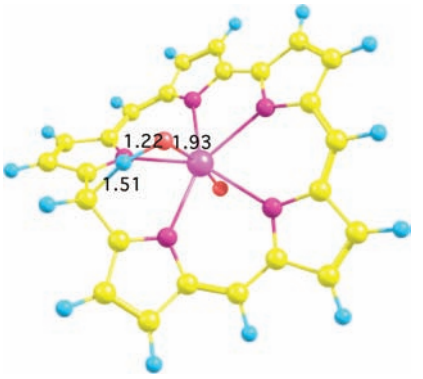

Figure 4. Transition state for **10a** to **8** isomerization, PBE/R3Z optimized geometry.

caused by its protonation. (The uranyl's uranium to oxygen bonds have partial triple character,[77] which makes them so stable. Protonation of a uranyl oxygen removes its lone pairs from bonding, thus weakening and elongating the U═O bond. The length of the HO−U bond is about 2 Å, versus about 1.8 Å in uranyl complexes.) The reason for the preference of the meso-CH isomers over the NH forms can be the same as for product **4**: better affinity of that ligand to the UO_2^{2+} due to the introduction of a tetrahedral C^{sp^3}, which contracts the ligand ring and thus allows for shorter U−N distances compared with the normal sapphyrin.

We note that a singlet configuration is the ground state for all the isomeric neutral complexes. The first triplet state is always of higher energy (Table 4). The PBE/L2 results do not differ significantly from PBE/R3Z. OLYP/L2 also preserves the order of isomers and their spin states. Inclusion of the solvation energies also does not alter the order. Therefore, it can be concluded that the oxidation state of uranium in all the complexes in Chart 3 is six.

These isomeric species can possibly be converted one into another either via intramolecular hydrogen shifts or through intermolecular processes via acid or base catalysis. The acid-catalyzed processes can be excluded due to the basic conditions of the experiment. Here we will consider intramolecular reaction pathways from the NH forms **7a** and **7b** to the OH form **8**, from it to the meso-CH isomer **10a**, and the 1,3-hydrogen shift from **7a** to **10a**. Structures of the corresponding transition states are presented in Figures 3−5, and their relative energies are provided in Table 4. Barriers for both transition states leading to the CH isomer are considerably higher than those for reactions involving NH and OH hydrogens, which is in agreement with general knowledge. A fairly recent DFT study[78] on the deprotonation reactions of CH, NH, and OH acids confirms that. Using the OLYP/L2 method leads to a uniform increase of activation barriers for all the interconversion transition states.

Probably, one cannot completely exclude the base-catalyzed intermolecular pathways of hydrogen migration. According to our COSMO results above, the anionic form **2** is found to be stable in solution. However, since CH acids are known to have higher activation barriers for the proton dissociation than OH and NH acids (see ref 78 and references therein), one could expect that the barriers for the intermolecular proton transfer mechanism pathways leading to the meso-CH forms **10a** and **10b** will be higher than those of NH and OH forms (and high in

absolute values). Therefore, while the meso-CH form **10a** is the most thermodynamically favorable form of all the isomeric neutral uranyl sapphyrin complexes, it might be hard to reach it starting from the NH forms that presumably form during the initial complexation of the uranyl cation with the ligand via the series of equilibria in eq 5.

5. MeOH Addition Step and Its Possible Intermediates. Initially, we considered the methanol addition step as it was proposed in the original experimental work, starting from the OH form of the uranyl sapphyrin complex **8** and yielding the complex **9**. Since the ground state of the complex **8** was found to be singlet, we attempted to locate the transition state on the singlet potential energy surface. The only solution found had non-Aufbau electron occupations, with the HOMO and LUMO energies of −0.1448 and −0.1481 atomic units, correspondingly. We tried then, to calculate a triplet TS starting from that structure and have found that it lies 4.7 kcal/mol below the singlet one (see Table S2, Supporting Information, for a complete list of the computed singlet and triplet state energies). The intermediate **9**, proposed in the original experimental work of Sessler et al.,[6] contains uranium in the formal oxidation state of four. Within the scalar relativistic approximation employed by us, the ground state for uranium(IV) is expected to be a high-spin triplet state since the unpaired electrons are occupying f-orbitals that are screened by the outermost valence shells and, thus, not susceptible to the influence of the ligand field. Indeed, the calculated intermediate **9** has a triplet ground state, just as the transition state leading to it. On the other hand, for the dioxouranium(VI) complexes, the ground state is singlet with the triplet state being an excited state corresponding to an electron transfer from a ligand. One can readily distinguish between these two cases based on the relative energies of the lowest singlet and triplet states, and the spin density localization, which should be predominantly on the metal for the U(IV) and on both the metal and the ligand for the U(VI).

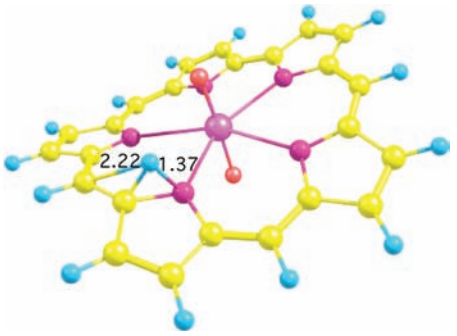

Figure 5. Transition state for **7a** to **10a** isomerization, PBE/R3Z optimized geometry; selected bond lengths in Å.

The intrinsic reaction coordinate (IRC) descent from the transition states on both the singlet and triplet surfaces leads to the corresponding singlet and triplet states of a prereaction complex of methanol with **8** and the complex **9**. The plots of the energies along the reaction coordinate for both singlet and triplet surfaces are shown in Figure 6. Together with the non-Aufbau electron occupations for the singlet TS, it shows that during the process, singlet−triplet crossing should happen. Here we note that for the real uranium complex, neither "singlet" nor "triplet" are strictly applicable terms because of the importance of the spin−orbit interactions. The scalar-relativistic DFT approximation that we use in this work does not allow us to study singlet−triplet crossing reactions directly. Still, from our scalar-relativistic calculations, we can identify the intermediate **9** and the TS(**8**−**9**) leading to it as complexes of uranium(IV). Here we take the relative energies of the triplet transition state and intermediate **9** with respect to the singlet state of **8** as an approximation to the activation barrier and the reaction energy, correspondingly.

Just as for the neutral source uranyl−sapphyrin complex, the isomer **7a** is not the only one possible, and the ONSH reaction intermediate can be imagined not only in form **9**. First, one would have to consider the possibility of the methanol addition to any of the isomeric neutral forms. For the synchronous

Table 5. Calculated Energies for Neutral Uranyl Sapphyrin Intermediate Complexes and Their Interconversion Transition States, Relative to the Singlet Ground State of 12a[a]

structure/spin state	PBE/R3Z	PBE/L2	OLYP/L2	PBE/ZORA TZP, gas phase	PBE/ZORA TZP pyridine solution
9/S	−2.2	−1.5	−0.2		
9/T	−11.1	−9.8	−11.1	−7.8	−7.9
12a/S	0.0	0.0	0.0	0.0	0.0
12a/T	1.2	2.4	−2.0		
12b/S	−8.6	−8.5	−8.7	−8.6	−8.6
12b/T	−7.0	−5.6	−9.8	−7.4	−9.3
12e/S	−12.5	−13.3	−21.0		
12e/T		0.5	−9.0		
13a/S	−25.0	−25.1	−23.7	−25.0	−24.0
13a/T		−7.6	−10.6		
13b/S	−28.4	−28.7	−35.9		
13b/T		−7.6	−10.6		
13c/S	−17.7	−18.0	−23.7		
13c/T		1.5	−4.0		
TS **9**−**13a**/T	14.8		16.2	15.9	15.9
TS **13a**−**13b**/S	9.2	9.3	15.3	10.5	12.5
TS **13a**−**13b**/T	13.5	14.8	16.2	14.0	13.8

[a] All values in kcal/mol.

dx.doi.org/10.1021/ja106566g |*J. Am. Chem. Soc.* 2011, 133, 4316–4329

monomolecular attack on the complex by neutral methanol, as assumed by us, two general types of pathways are possible: Type I, with the proton of methanol going to one of the uranyl oxygens, and Type II, where it goes to the neighboring pyrrolic nitrogen. Corresponding transition states (TS) of the Types I and II are shown schematically in Scheme 2.

Scheme 2. Two Types of Transition States for the Methanol Addition Step Considered in This Work: Type I Includes Protonation of the Uranyl Oxygen and Type II of the Neighboring N4 Atom

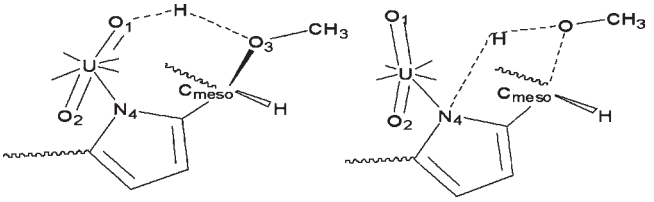

Chart 4. Possible Neutral (9, 12a−e, 13a,b) Intermediates for Methanol Addition

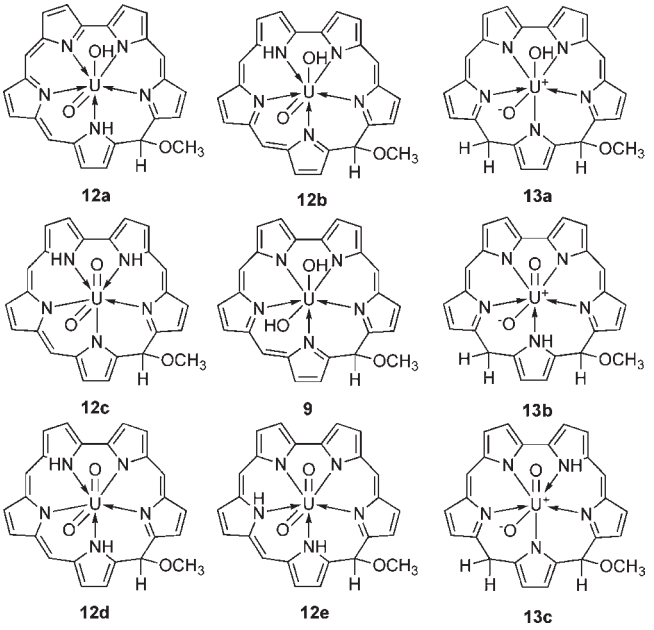

Starting from each of the neutral isomers, **7a−c**, **8**, **10a,b**, we could build pathways via transition states I and II, leading to the addition of the methoxy group to the C_{meso1}, and of the proton, either to the uranyl oxygen or to the N4 (Scheme 1 for the numeration of atoms). This generates a multitude of neutral intermediate complexes (selectively) listed in the Chart 4; relationships between the starting complexes and the intermediates are shown in Scheme 3. For example, the intermediate **9** arises as a result of a process of Type I starting at the neutral isomeric complex **8**. The result of a process of Type II for complex **8** will be the complex **12a** (Chart 4); addition of the methanol to the NH form **7b** generates isomers **12b** and **12d**, correspondingly.

These isomeric intermediates (**9**, **12a−d**, **13a−c**) might transform one into another via proton-shift reactions similar to those described above for the neutral uranyl sapphyrins **7a−c**, **8**, and **10a,b**. Moreover, due to the possibility of the presence of the anionic form **2** in pyridine solution, one has to consider the addition of methanol to it via both Type I and II pathways as well, leading to adducts **11a** or **11e**, respectively, which could possibly isomerize to **11b−d** or get deprotonated further to the dianionic adduct form **14** (Chart 5). Finally, the neutral intermediates, **9**, **12a−c**, and **13a,b**, can be deprotonated, yielding **11a−d** and then **14**.

Relative energies of neutral and ionic isomers of the intermediates are presented in the Tables 5 and 6, correspondingly. We can rely on the observation that the rules of stability for the intermediates are the same as for neutral source complexes. That is, the order of stabilities is determined entirely by the position of protons (there are two of them in the neutral intermediates and one in the monoanionic forms) in the complexes: the meso-CH forms are preferable, followed by the NH forms, and the least stable are the uranyl OH-protonated isomers (Table 5). Energies and geometries of all the structures **11−14** are provided in the Supporting Information. Transition states are shown for the anionic pathway including **2** and the Type I TS and Type II TS resulting from it (Figures 7 and 8).

Both Type I and Type II reactions were calculated for the anion **2**, as well as for neutral NH form **7b** and OH form **8**, for the singlet PES. The Type II pathway for all these cases was found to

Scheme 3. Relationships between Uranyl−Sapphyrin Complexes and Methanol Addition Intermediates Resulting from TS Type I and II

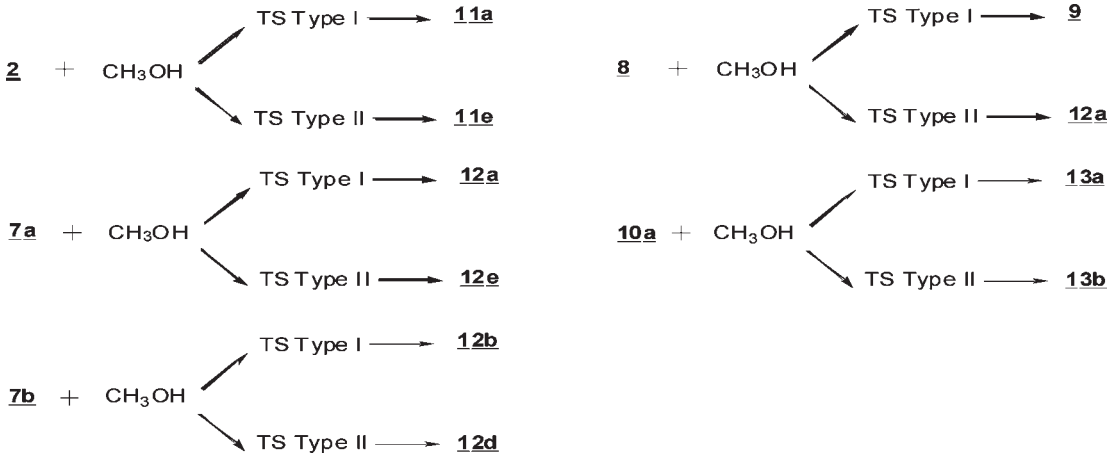

dx.doi.org/10.1021/ja106566g |J. Am. Chem. Soc. 2011, 133, 4316–4329

Chart 5. Possible Anionic (11a−c) Intermediates for Methanol Addition

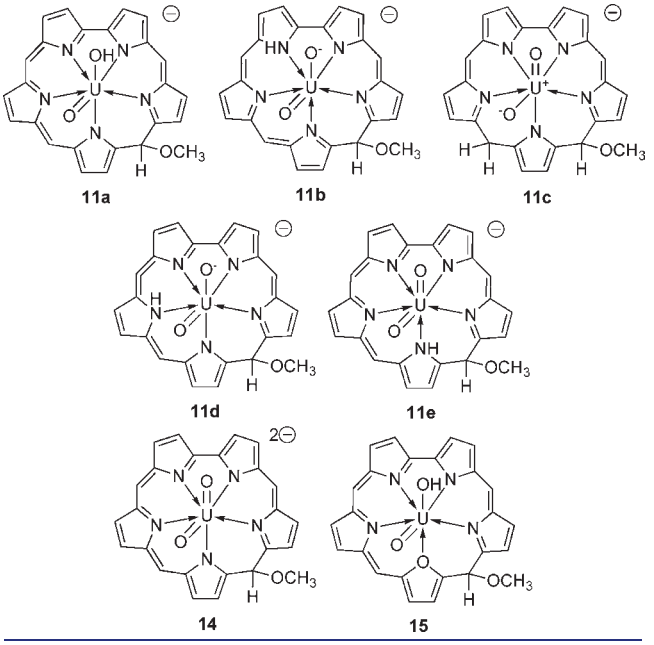

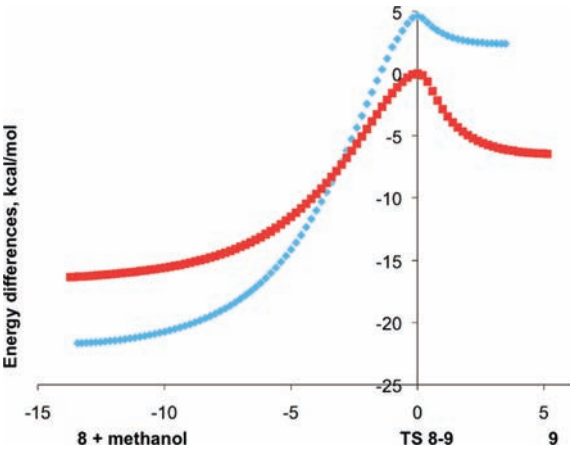

Figure 6. Calculated intrinsic reaction coordinate paths for triplet (red squares) and singlet (blue diamonds) potential energy surfaces for methanol addition to complex **8** yielding **9**. Reaction coordinate in bohr·(a.m.u)$^{1/2}$

be less favorable than Type I. Probably, this result will hold for any other isomer, so we did not attempt to probe it any further. Below we will consider closely only Type I TS involving the protonation of the uranyl oxygen.

In addition to the singlet pathway, for reactions of the neutral NH form **7b**, the CH form **10a**, and the anion **2**, saddle points were located on the triplet PES. Unlike the OH form **8**, for these NH and CH forms, the singlet TS as well as the products were the stable solutions. The corresponding triplet transition states are of considerably higher energy than the singlet ones; for intermediates, the difference is not big (about 1−1.5 kcal/mol) but still in favor of the singlet. Above, we concluded that the intermediate **9** is a complex of U(IV) based on its geometry and triplet nature with two unpaired electrons located at the uranium atom. For **11a**, **12b**, and **13a**, on the basis of their singlet character and their geometry of the uranyl moiety, we could conclude that they are compounds

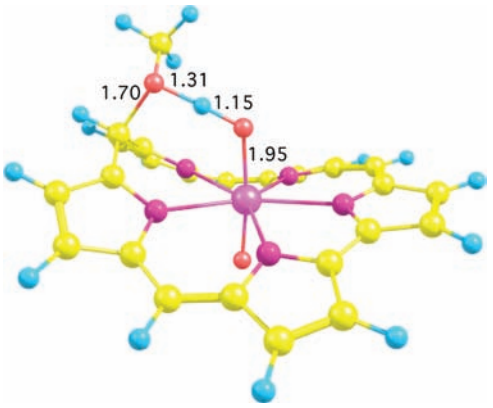

Figure 7. Transition state Type I for methanol addition to anion complex **2**, PBE/R3Z optimized geometry; selected bond lengths in Å.

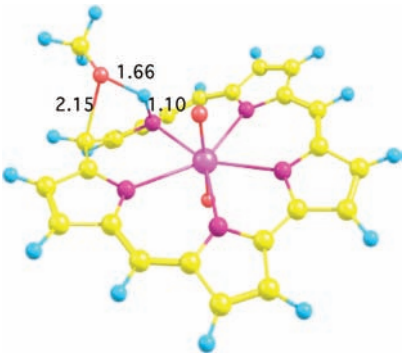

Figure 8. Transition state Type II for methanol addition to anion complex **2**, PBE/R3Z optimized geometry; selected bond lengths in Å.

of U(VI). Because sapphyrin and oxasapphyrin are shown above to be similar with respect to complexation energies, we have also considered the addition of methanol to the latter (**3**) using a TS of Type I, leading to the structure **15** (Chart 5), on the singlet PES.

Considering the results from different density functionals, we note that in contrast to the source complexes for the intermediates, both neutral and anionic, the OLYP/L2 method favors the triplet state stronger than PBE. For the compound **9**, the triplet is significantly more stable for both functionals. However, for the neutral intermediate **12a** and anionic **11a**, the order of states depends on the choice of density functional. The OLYP method predicts the ground state of the two latter to be triplet, while PBE predicts the singlet−triplet splitting to be about 2 kcal/mol for both of the methods. However, all the functionals find that the most stable isomers of them are singlets, **13a**, **13b**, and **11c**.

Next, let us consider the energies and activation barriers of the methanol addition step for the isomeric neutral forms **7b**, **8**, and **10a** and the anionic form **2**, as summarized in the Table 5. First, we note that all these reactions are endothermic; the driving force of the substitution comes from the next step, the oxidation of the intermediate by molecular oxygen. However, among the neutral species, the triplet intermediate **9** (OH-protonated pathway) is the least exoergic, followed closely by **13a** (CH-protonated pathway). For the latter, the activation barrier is the smallest from all the compounds considered. This can be explained as follows: the isomer **13a** has a conjugated π-system already broken by CH protonation, so an incoming MeOH does not have to pay an additional energetic penalty for its breaking.

dx.doi.org/10.1021/ja106566g |*J. Am. Chem. Soc.* 2011, 133, 4316–4329

Scheme 4. Calculated PBE/R3Z Gibbs free energy profile, in COSMO pyridine solution, for selected neutral and anionic reaction pathways, kcal/mol. [a]

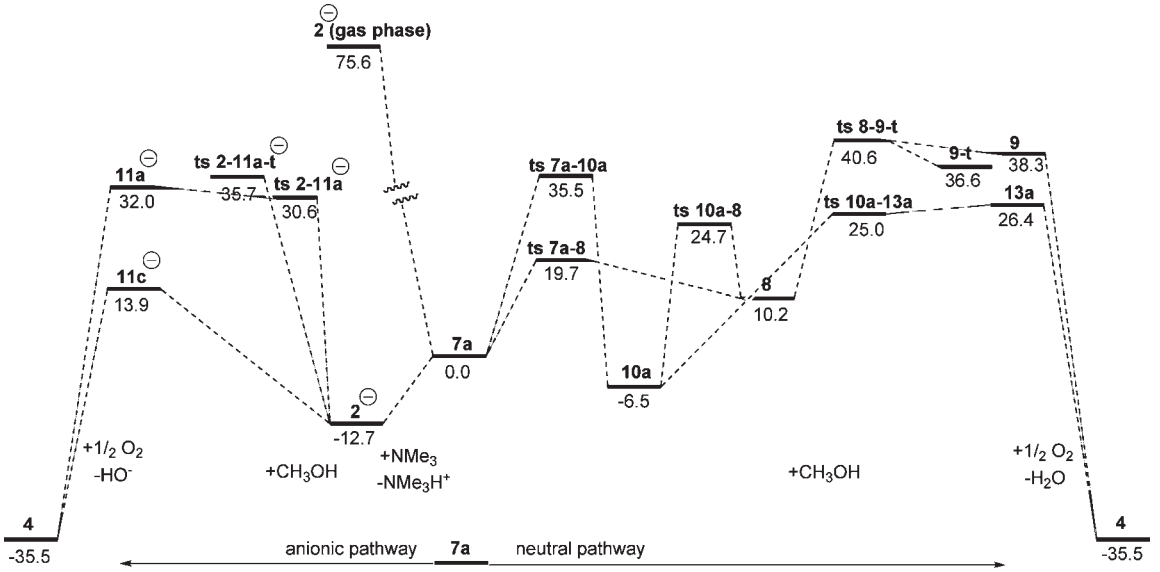

[a] See Charts 2−5 for the numeration of the complexes. Suffix "-t" denotes triplet states of the complex, otherwise singlet.

As compared with these OH and CH cases, there is no significant difference in methoxylation energies and activation barriers between the NH-protonated (**7b**) and anionic (**2**) forms of the uranyl−sapphyrin complex; moreover, the oxasapphyrin **3** yields compound **15** with similar energies. Thus we conclude that it is the state of uranyl (protonated vs nonprotonated) and the shape of the ligand (intact conjugated sapphyrin vs buckled CH form of it) that play a major role for this reaction, but not the ligand's charge (nor even its donor atoms; the oxa-substitution does not change the picture.) Therefore, the overall charge of the complex can be important for solvation effects (for charged species have higher solvation energies than neutral ones in polar solvents) but not for the barrier of the methanol addition reaction. The OLYP functionals always predict significantly larger activation barriers for the transition states compared with PBE.

Selected PES profiles are shown in Scheme 4. From Table 7, we see that the methanol insertion step has the lowest activation barrier and is the least exothermic for the CH form **10a.** The formation of the complex **10a** from either the NH or OH forms (**7a**−**c** and **8**, correspondingly) has a large activation barrier (Table 5). For the insertion intermediates **11a**, **b**, **12a**−**c**, and **13**, the latter bis-CH form is the most stable, but conversions from other isomers are also likely to have significant activation barriers. We have calculated it for one case of conversion of **8** to **11a**; it has activation energies of 24.5 and 20.3 kcal/mol on the triplet and singlet potential energy surfaces, correspondingly.

The next best methanol insertion path is the one starting from the OH form **8**, yielding the U(IV) intermediate **9**. Formation of **8** from **7a**−**c** has a rather small activation barrier, but **8** is the least stable isomer of all neutral forms and its instability adds to the overall reaction barrier (16.5 + 10.1 = 26.6 kcal/mol). For the NH orm **7b**, the barrier is 23.7 kcal/mol, but the reaction is more endoergic than for any of the other forms. The barrier for reverse reaction to methanol addition is the largest one for the OH path (that is, elimination of CH_3OH from **9** yielding **8**), which makes this path consistent with the experimental observation of a stable intermediate under airless conditions.[6]

Our scalar-relativistic calculations do not include spin−orbit interactions, which should stabilize U(IV) systems having two unpaired f-electrons by up to a few kcal/mol.[22] We have computed selected single point energies including spin−orbit effects and found that **9** is stabilized compared with **8**, but the effect does not exceed 2 kcal/mol (see the Supporting Information, Table S4); the compound **8** is also slightly stabilized by the spin−orbit compared with the isomer **7a**.

Above, in the discussion on the overall reaction thermodynamics and stability, we have calculated the solvation energies for **2** and **7** (Table 3). From the solvation data (Tables 4,5, and 6) it was shown that isomeric forms of the source uranyl sapphyrin complexes (**8**, **7a**−**c**, **10a**,**b**), the methoxylated intermediates (**9**, **12b**−**c**, **13a**), and the transition states between them have close solvation-free energies for a given charge of the complex. The change to the mechanism that is due to solvation is the differentiation between neutral (**7a**−**c**, **8**, **10a**,**b**) and anionic pathways by stabilizing the latter. As the protons most likely to go are the U═O−H ones from **8** and NH from **7a**−**c**, the pathway then has to be anionic and singlet, from **2** to **11a**. Thus while in the gas phase, the U(IV) pathway via neutral intermediate **9** is favorable. Inclusion of the solvation energies makes anionic singlet (that is, U(VI)) pathways preferred.

The solvation effects might also stabilize methoxylated intermediates (which have two protons for the neutral and one for the anionic paths) by deprotonizing them, ultimately leading to the dianion **14**. We consider the corresponding intermediate deprotonation processes (eqs and) in Table 3. Deprotonation of the neutral intermediate **11a** with formation of **12a** in solution is strongly thermodynamically favored; further deprotonation to **14** is slightly endoergic, almost thermoneutral.

The final stage of the reaction is oxidation of an intermediate by molecular oxygen. Two following example cases have been considered: oxidation of the neutral complex **12a**, which involves

dx.doi.org/10.1021/ja106566g |*J. Am. Chem. Soc.* 2011, 133, 4316–4329

Table 6. Calculated Energies for Anionic Uranyl−Sapphyrin Intermediate Complexes and Relative to the Singlet Ground State of 11b[a]

structure/spin state	PBE/R3Z	PBE/L2	OLYP/L2	PBE/ZORA TZP, gas phase	PBE/ZORA TZP pyridine solution
11a/S	−0.8	0.0	5.6	1.3	3.4
11a/T	0.6	2.9	3.7		
11b/S	0.0	0.0	0.0	0.0	0.0
11b/T		12.0	10.1		
11c/S	−17.2	−16.8	−16.8	−16.7	−17.0
11c/T		7.9	7.9		
11d/S	−4.2	−4.3	−4.6	−4.2	−4.2
11d/T		12.9	9.9		
11e/S	−3.6	−3s.7	−4.8	−3.7	−5.1
11e/T		10.7	7.1		

[a] All values in kcal/mol.

Table 7. Energies of Activation (E_a) and Reaction (ΔE) of the Methanol Addition Step for Selected Reaction Pathways, Relative to the Most Stable Spin State of the Reagent[a]

reaction				E_a				ΔE			
reagents	TS	product	spin mult.	PBE/R3Z, gas phase	PBE/L2, gas phase	OLYP/L2, gas phase	PBE/L2, pyridine	PBE/R3Z, gas phase	PBE/L2, gas phase	OLYP/L2, gas phase	PBE/L2, pyridine
2 + MeOH	Type I	**11a**	S	27.6	28.0	45.8	32.6	25.3	25.6	42.0	31.8
2 + MeOH	Type I	**11a**	T	37.7	39.4	53.3	40.1	26.7	28.5	40.1	26.6
2 + MeOH	Type II	**11b**	S	41.5				22.4			
7b + MeOH	Type I	**12b**	S	23.7	23.7	41.0	28.1	22.3	22.4	38.4	27.4
7b + MeOH	Type I	**12b**	T	34.6	35.4	50.5	33.1	23.9	25.4	37.3	28.4
7b + MeOH	Type II	**12d**	S	41.5	41.6	53.9	44.8	20.9			
8 + MeOH	Type I	**9**	S	21.1	21.4	36.3		18.8	19.4	32.3	
8 + MeOH	Type I	**9**	T	16.5	17.7	30.0	20.6	10.0	11.1	21.4	14.9
8 + MeOH	Type II	**12a**	S	39.5	39.7	50.1	42.1	21.1	20.9	32.6	24.9
10a + MeOH	Type I	**13a**	S	13.5	13.0	30.8	18.8	13.2	12.7	30.2	19.6
10a + MeOH	Type I	**13a**	T					29.6	30.3	43.3	
3 + MeOH	Type I	**15**	S	27.9	27.5	46.3		25.4	25.1	42.2	
3 + MeOH	Type I	**15**	T	39.9							

[a] All values in kcal/mol.

removal of the two hydrogens, and the oxidation of the dianion **14a**, which just changes its overall charge in order to turn into the product **4**. Both processes (eqs and , Table 3, correspondingly) are strongly exoergic in both gas phase and solution. We would like to note that, while the end result is the same, for a noninnocent path involving a triplet intermediate (**9**) the oxidation of U(IV) occurs, while for innocent anionic pathways, it is the sapphyrin ligand that gets oxidized by changing its charge or losing hydrogen atoms.

CONCLUSIONS

In this paper, we applied scalar-relativistic DFT to model uranyl−sapphyrin complexes and their oxidative nucleophilic substitution (ONSH) with methanol. We also have studied the mechanistic details of the ONSH, investigating whether uranium plays a noninnocent role of the primary oxidant or just acts as an electron-withdrawing observer "group" promoting the regular ONSH mechanism.

The computational method has shown good agreement with experimental geometries and vibrational frequencies for oxasapphyrin and methoxylated sapphyrin−uranyl complexes (**3** and **4**, correspondingly), with slight overestimation of uranium to ligand bond lengths, which is common for GGA DFT.

The interactions of uranyl with the sapphyrin di- and trianions, as well as with methoxylated sapphyrin dianion and oxasapphyrin, were analyzed using the ETS energy decomposition procedure. Based on its results, we see that changes in the size of sapphyrin's macrocyclic inner cavity due to methoxylation (by introducing a tetrahedral carbon in one of the meso-bridges) make its binding with the uranyl ion stronger. This constitutes the driving force for the hydrogen-to-methoxy-group substitution process and pays off for the breaking of the aromaticity of the ligand.

The failure of uranyl to form a 1:1 complex with sapphyrin was ascribed to the trianionic character of the latter; the uranium complex will have either an overall charge, as in **2** (and thus cannot be stabilized as a solid, at least with the counterion available in the original experimental work) or be in various protonated forms that are less stable due to unfavorable metal-to-ligand interactions where they are protonated (NH forms **7a**−**c**) or destabilized by uranyl protonation (the OH form **8**). Interestingly, the sapphyrin−uranyl complexes have a set of stable isomers similar to transition metal−corrole complexes, with one of the hydrogens going to the meso-carbon bridge. However, according to our calculations, their formation via proton migration is kinetically disfavored.

The scalar-relativistic DFT calculations we employed did show that, at this level of theory, a "noninnocent" path involving the reduction of uranyl to U(IV) does exist. However, this path is not related to a higher charge on the sapphyrin ligand (the anionic pathway via **2** was found to be a singlet one) but rather

dx.doi.org/10.1021/ja106566g |J. Am. Chem. Soc. 2011, 133, 4316–4329

has to be assisted by protonation of the uranyl (it goes through the OH form **8** only). In the gas phase, this path is competitive against "innocent" pathways with other neutral uranyl−sapphyrin complexes (CH and NH forms, correspondingly). However, taking solvation into account makes the "innocent" anionic path corresponding to the regular ONSH more favorable because solvation in a polar solvent stabilizes the charged species.

This interesting example of unusual reactivity of a uranyl−expanded porphyrin complex clearly asks for more studies, experimental as well as theoretical.

■ ASSOCIATED CONTENT

Supporting Information. Geometries of reactants, products, and transition states computed at the PBE/R3Z level of theory; total energies of the complexes calculated by Priroda and ADF programs; details of the R3Z basis sets used in this work; comparison of single point and COSMO-optimized energies, as well as spin−orbit energies for selected complexes; and complete refs 57 and 62. This material is available free of charge via the Internet at http://pubs.acs.org.

■ AUTHOR INFORMATION

Corresponding Author
*E-mail: gas5x@yahoo.com

■ ACKNOWLEDGMENT

The author thanks Dr. D. N. Laikov, Moscow State University, for providing him with the Priroda code and basis sets. The author is grateful to Prof. H. Georg Schreckenbach for his critical reading of earlier versions of the manuscript, as well as for help with the ADF computations.

■ REFERENCES

(1) Sessler, J. L. *Expanded, Contracted & Isomeric Porphyrins*; Pergamon Press: New York, 1997.
(2) Sessler, J. L.; Vivian, A. E.; Seidel, D.; Burrell, A. K.; Hoehner, M.; Mody, T. D.; Gebauer, A.; Weghorn, S. J.; Lynch, V. *Coord. Chem. Rev.* **2001**, *216*, 411.
(3) Sessler, J. L.; Gorden, A. E. V.; Seidel, D.; Hannah, S.; Lynch, V.; Gordon, P. L.; Donohoe, R. J.; Tait, C. D.; Keogh, D. W. *Inorg. Chim. Acta* **2002**, *341*, 54.
(4) We use the Sessler's nomenclature for expanded porphyrins; it is provided in refs 1−3.
(5) Woodward, R. B. *Special Publication* **1966**, 21.
(6) Burrell, A. K.; Cyr, M. J.; Lynch, V.; Sessler, J. L. *J. Chem. Soc., Chem. Commun.* **1991**, 1710.
(7) Sessler, J. L.; Gebauer, A.; Hoehner, M. C.; Lynch, V. *Chem. Commun.* **1998**, 1835.
(8) Makosza, M.; Wojciechowski, K. *Chem. Rev.* **2004**, *104*, 2631.
(9) Arnold, P. L.; Patel, D.; Wilson, C.; Love, J. B. *Nature* **2008**, *451*, 315.
(10) Yahia, A.; Arnold, P. L.; Love, J. B.; Maron, L. *Chem. Commun.* **2009**, 2402.
(11) Yahia, A.; Arnold, P. L.; Love, J. B.; Maron, L. *Chem.—Eur. J.* **2010**, *16*, 4881.
(12) Fortier, S.; Wu, G.; Hayton, T. W. *J. Am. Chem. Soc.* **2010**, *132*, 6888.
(13) Fortier, S.; Hayton, T. W. *Coord. Chem. Rev.* **2010**, *254*, 197.
(14) Hayton, T. W. *Dalton Trans.* **2010**, *39*, 1145.
(15) Arnold, P. L. *Nat. Chem.* **2009**, *1*, 29.
(16) Fox, A. R.; Arnold, P. L.; Cummins, C. C. *J. Am. Chem. Soc.* **2010**, *132*, 3250.
(17) Schnaars, D. D.; Wu, G.; Hayton, T. W. *J. Am. Chem. Soc.* **2009**, *131*, 17532.
(18) Schreckenbach, G.; Hay, P. J.; Martin, R. L. *J. Comput. Chem.* **1999**, *20*, 70.
(19) Kaltsoyannis, N.; Hay, P. J.; Li, J.; Blaudeau, J. P.; Bursten, B. E. In *The Chemistry of the Actinide and Transactinide Elements*, 3rd ed.; Morss, L. R., Edelstein, N. M., Fuger, J., Katz, J. J., Eds.; Springer: Dordrecht, The Netherlands, 2006; Vol. 3, p 1893.
(20) Koch, W.; Holthausen, M. C. *A Chemist's Guide to Density Functional Theory*; Wiley Verlag Chemie: New York, 2000.
(21) Clavaguera-Sarrio, C.; Vallet, V.; Maynau, D.; Marsden, C. J. *J. Chem. Phys.* **2004**, *121*, 5312.
(22) Batista, E. R.; Martin, R. L.; Hay, P. J. *J. Chem. Phys.* **2004**, *121*, 11104.
(23) Shamov, G. A.; Schreckenbach, G.; Vo, T. *Chem.—Eur. J.* **2007**, *13*, 4932.
(24) Shamov, G. A.; Schreckenbach, G.; Martin, R. L.; Hay, P. J. *Inorg. Chem.* **2008**, *47*, 1465.
(25) Pan, Q. J.; Shamov, G. A.; Schreckenbach, G. *Chem.—Eur. J.* **2010**, *16*, 2282.
(26) Laikov, D. N., Priroda code.
(27) Laikov, D. N.; Ustynyuk, Y. A. *Russ. Chem. Bull.* **2005**, *54*, 820.
(28) Laikov, D. N. Presented at the DFT2000 Conference, Menton, France, 2000.
(29) Dyall, K. G. *J. Chem. Phys.* **1994**, *100*, 2118.
(30) Perdew, J. P.; Burke, K.; Ernzerhof, M. *Phys. Rev. Lett.* **1996**, *77*, 3865.
(31) Eichkorn, K.; Treutler, O.; Ohm, H.; Haser, M.; Ahlrichs, R. *Chem. Phys. Lett.* **1995**, *240*, 283.
(32) Laikov, D. N. *Chem. Phys. Lett.* **1997**, *281*, 151.
(33) Guell, M.; Luis, J. M.; Sola, M.; Swart, M. *J. Phys. Chem. A* **2008**, *112*, 6384.
(34) Swart, M. *J. Chem. Theory Comput.* **2008**, *4*, 2057.
(35) Swart, M.; Guell, M.; Luis, J. M.; Sola, M. *J. Phys. Chem. A* **2010**, *114*, 7191.
(36) Handy, N. C.; Cohen, A. J. *Mol. Phys.* **2001**, *99*, 403.
(37) Conradie, J.; Ghosh, A. *J. Phys. Chem. B* **2007**, *111*, 12621.
(38) Conradie, J.; Ghosh, A. *J. Chem. Theory Comput.* **2007**, *3*, 689.
(39) Guell, M.; Sola, M.; Swart, M. *Polyhedron* **2010**, *29*, 84.
(40) Hoe, W. M.; Cohen, A. J.; Handy, N. C. *Chem. Phys. Lett.* **2001**, *341*, 319.
(41) Laikov, D. N. *Chem. Phys. Lett.* **2005**, *416*, 116.
(42) Berard, J. J.; Shamov, G. A.; Schreckenbach, G. *J. Phys. Chem. A* **2007**, *111*, 10789.
(43) Shamov, G. A.; Schreckenbach, G. *J. Phys. Chem. A* **2005**, *109*, 10961.
(44) Shamov, G. A.; Schreckenbach, G. *J. Am. Chem. Soc.* **2008**, *130*, 13735.
(45) Shamov, G. A.; Schreckenbach, G. *Inorg. Chem.* **2008**, *47*, 805.
(46) Shamov, G. A.; Schreckenbach, G. *J. Phys. Chem. A* **2006**, *110*, 9486.
(47) Berard, J. J.; Schreckenbach, G.; Arnold, P. L.; Patel, D.; Love, J. B. *Inorg. Chem.* **2008**, *47*, 11583.
(48) Schreckenbach, G.; Shamov, G. A. *Acc. Chem. Res.* **2010**, *43*, 19.
(49) Odoh, S. O.; Schreckenbach, G. *J. Phys. Chem. A* **2010**, *114*, 1957.
(50) Morokuma, K.; Kitaura, K. In *Chemical Applications of Atomic and Molecular Electrostatic Potentials*; Politzer, P., Truhlar, D. G., Eds.; Plenum: New York, 1981; p 215.
(51) Ziegler, T.; Rauk, A. *Theor. Chim. Acta* **1977**, *46*, 1.
(52) Ziegler, T.; Rauk, A. *Inorg. Chem.* **1979**, *18*, 1558.
(53) Bickelhaupt, F. M.; Baerends, E. J. In *Reviews in Computational Chemistry*; Wiley: New York, 2000; Vol. 15, p 1.
(54) te Velde, G.; Bickelhaupt, F. M.; Baerends, E. J.; Guerra, C. F.; Van Gisbergen, S. J. A.; Snijders, J. G.; Ziegler, T. *J. Comput. Chem.* **2001**, *22*, 931.
(55) Fonseca Guerra, C.; Visser, O.; Snijders, J. G.; te Velde, G.; Baerends, E. J. In *Methods and Techniques in Computational Chemistry METECC-95*; Clementi, E., Corongiu, C., Eds.; STEF: Cagliari, Italy, 1995; p 305.

(56) Fonseca Guerra, C.; Snijders, J. G.; te Velde, G.; Baerends, E. J. *Theor. Chem. Acc.* **1998**, *99*, 391.
(57) Baerends, E. J. et al. ; *Scientific Computing and Modelling, Theoretical Chemistry*; Vrije Universiteit: Amsterdam, The Netherlands, 2010.
(58) van Lenthe, E.; Baerends, E. J.; Snijders, J. G. *J. Chem. Phys.* **1993**, *99*, 4597.
(59) van Lenthe, E.; Baerends, E. J.; Snijders, J. G. *J. Chem. Phys.* **1994**, *101*, 9783.
(60) van Lenthe, E.; Ehlers, A.; Baerends, E. J. *J. Chem. Phys.* **1999**, *110*, 8943.
(61) van Lenthe, E.; Baerends, E. J. *J. Comput. Chem.* **2003**, *24*, 1142.
(62) Baerends, E. J. et al. ; *Scientific Computing and Modelling, Theoretical Chemistry*; Vrije Universiteit: Amsterdam, The Netherlands, 2004.
(63) Eschrig, H.; Servedio, V. D. P. *J. Comput. Chem.* **1999**, *20*, 23.
(64) van Wullen, C. *J. Comput. Chem.* **2002**, *23*, 779.
(65) vanLenthe, E.; Snijders, J. G.; Baerends, E. J. *J. Chem. Phys.* **1996**, *105*, 6505.
(66) vanLenthe, E.; vanLeeuwen, R.; Baerends, E. J.; Snijders, J. G. *Int. J. Quantum Chem.* **1996**, *57*, 281.
(67) Klamt, A.; Schüürmann, G. *J. Chem. Soc., Perkin Trans. 2* **1993**, 799.
(68) Pye, C. C.; Ziegler, T. *Theor. Chem. Acc.* **1999**, *101*, 396.
(69) Klamt, A.; Jonas, V.; Bürger, T.; Lohrenz, J. C. W. *J. Phys. Chem. A* **1998**, *102*, 5074.
(70) Szterenberg, L.; Latos-Grazynski, L. *J. Phys. Chem. A* **1999**, *103*, 3302.
(71) Ernzerhof, M.; Scuseria, G. E. *J. Chem. Phys.* **1999**, *110*, 5029.
(72) Jensen, F. *J. Chem. Theory Comput* **2010**, *6*, 2726.
(73) Hambright, P. In *Porphyrins and Metalloporphyrins*; Smith, K. M., Ed.; Elsevier: New York, 1975; p 234.
(74) Roos, B. O.; Veryazov, V.; Conradie, J.; Taylor, P. R.; Ghosh, A. *J. Phys. Chem. B* **2008**, *112*, 14099.
(75) Ghosh, A. *J. Biol. Inorg. Chem.* **2006**, *11*, 712.
(76) Ghosh, A.; Steene, E. *J. Inorg. Biochem.* **2002**, *91*, 423.
(77) Dyall, K. G. *Mol. Phys.* **1999**, *96*, 511.
(78) Keeffe, J. R.; Gronert, S.; Colvin, M. E.; Tran, N. L. *J. Am. Chem. Soc.* **2003**, *125*, 11730.

■ NOTE ADDED AFTER ASAP PUBLICATION

Due to a production error, Table 3 was published with errors on March 7, 2011. The corrected version was reposted on March 23, 2011.